physical sciences forum

MDPI

Proceeding Paper

Fast Method for the Measurement of Dispersion of Integrated Waveguides by Utilizing Michelson Interferometry Effects †

Isaac Yorke [1,2,*], Lars Emil Gutt [2], Peter David Girouard [3] and Michael Galili [2]

[1] Department of Engineering and Architecture, University of Parma, Parco Area delle Scienze 181/A, I-43124 Parma, Italy
[2] Department of Electrical and Photonics Engineering, Technical University of Denmark, Ørsteds Plads Bygning, 3402800 Kongens Lyngby, Denmark; lgutt@dtu.dk (L.E.G.); mgal@dtu.dk (M.G.)
[3] IMEC-NL Holst Centre, 5656 AE Eindhoven, The Netherlands; peter.girouard@imec.nl
* Correspondence: isaac.yorke@unipr.it; Tel.: +39-328-773-8937

† Presented at 1st International Online Conference on Photonics, 14–16 October 2024; Available online: https://sciforum.net/event/IOCP2024.

Abstract: In this paper we demonstrate a new approach to the measurement of dispersion of light reflected in integrated optical devices. The approach utilizes the fact that light reflected from the end facet of an integrated waveguide will interfere with light reflected from points inside the device under test (DUT), effectively creating a Michelson interferometer. The distance between the measured fringes of this interferometric signal will depend directly on the group delay experienced in the device under test, allowing for fast and easy measurement of waveguide dispersion. This approach has been used to determine the dispersion of a fabricated linearly chirped Bragg gratings waveguide and the result agrees well with the designed value.

Keywords: Michelson interferometer; chirped Bragg gratings; group delay; dispersion; waveguide

1. Introduction

Many methods for the measurement of the dispersion on integrated waveguides exists. An often used method is the phase shift technique [1], where the dispersion of a device can be extracted by modulating a laser and directly measuring the phase delay of a measured RF signal by using a vector network analyzer (VNA). Alternatively, interferometric approaches can be used, such as the method presented by K. R. H. Bottril et al. [2], where a programmable optical filter is utilized to control the phase written to a sideband of a RF modulated laser and interfering this with a reference band after propagation through an optical device. By varying this controllable phase, the phase shift experienced by light propagating through an optical component can be recovered and the dispersion calculated. Both of these techniques are limited by the modulation frequencies used and by requiring access to specialized equipment such as VNAs and programmable optical filters. In this paper, we propose a new method that can be used for the case of integrated optical waveguides, which sidesteps some of the requirements of other methods. The method is based on the fact that when coupling to an integrated waveguide using edge coupling, some fraction of the light sent to the waveguide will be reflected at the edge of the chip. Other light will be coupled into the waveguide and later reflected, for instance by a Bragg grating. As the reflected light exits the waveguide, it will be recombined with the field that is initially reflected, creating a Michelson interferometer, which will have an interference fringe spacing which depends on the group delay experienced by the light reflected on-chip. Typically, interferometric techniques like this are impractical since they depend on the mutual coherency between the light taking two different paths. In the case of integrated optics, this is not a limitation though, as parameters such as the polarization are much more stable in integrated photonics, especially within high index contrast waveguides like

Citation: Yorke, I.; Gutt, L.E.; Girouard, P.D.; Galili, M. Fast Method for the Measurement of Dispersion of Integrated Waveguides by Utilizing Michelson Interferometry Effects. *Phys. Sci. Forum* **2024**, *10*, 4. https://doi.org/10.3390/psf2024010004

Academic Editor: Anna Łukowiak

Published: 20 December 2024

silicon on insulator. Interferometer configurations such as Michelson and Fabry Perot can be realized using uniform or chirped Bragg gratings acting as partial reflectors [3]. The combined intensity (I) contained in the two beams reflected from the mirrors of Michelson interferometer is given by:

$$I = |E_1 \exp[i(kz + \omega t + \phi_1)] + E_2 \exp[i(kz + \omega t + \phi_2)]|^2 \quad (1)$$

ω represents the angular frequency, $k = 2\pi/\lambda$ represents the wavenumber, λ represents the wavelength, ϕ_n represents the grating chirp and is a function of position (z) and time (t). E_1 and E_2 are the amplitudes of the two beams [4]. Since the group delay of an electric field is:

$$\tau = \frac{\partial \phi}{\partial \omega}, \quad (2)$$

the group delay experienced by the field can be extracted by recovering the phase of the interference fringes [1,5]. Alternatively, if we think of this system as a Fabry-Perot cavity with a free spectral range (FSR) of Δf, the group delay for one round trip is inversely proportional to Δf [5]. Thus;

$$\tau = \frac{1}{\Delta f} \quad (3)$$

So, by finding the spacing between interference fringes we can find the group delay using this method.

2. Method

In Figure 1a, the experimental setup used to measure dispersion is shown. In this setup, light is coupled to the DUT through a circulator and the light that is reflected from it is recorded on a power meter. Simultaneously, some of the light is coupled to a free space cavity with an FSR of 100 MHz, with the transmission through this cavity also being recorded on a photo-detector. As the wavelength of the laser is swept, the light reflected from the DUT and the light transmitted through the free space cavity are recorded simultaneously on an oscilloscope, such that the transmission through the free space cavity can be used as a frequency reference, as the resonance have a well known frequency spacing. The output from the free space cavity is used to correct the inaccuracies in the tunable laser's wavelength sweeping. This involves aligning the known frequency spacing of the free space cavity with corresponding peaks or features in the tunable laser's trigger output signal. Figure 1b shows the plot of the reflected spectrum versus frequency obtained from one of the DUT.

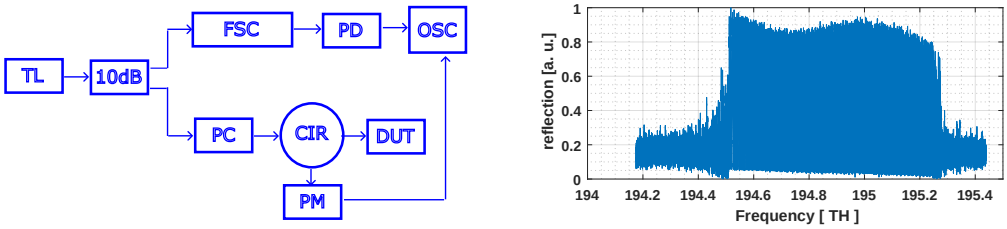

(**a**) (**b**)

Figure 1. (**a**) Experimental setup to measure the reflected spectrum. TL: Tunable Laser, 10 dB: 10 dB coupler, FSC: Free Space Cavity, PD: Photo Detector, PC: Polarization Controller, CIR: Circulator, PM: Power meter, OSC: Oscilloscope, DUT: Device under test. (**b**) Reflected spectrum as a function of frequency [TH], obtained from the example device under analysis.

The robustness of our model rest on the Savitzky Golay filter (SGF), which is a peak preservation filter. This filter is proven to be equivalent to discrete convolution with fixed

impulse response. Originally proposed to smoothing noisy data obtained from chemical spectrum analyzers, this filter has been used to demonstrate that least square smoothing reduces noise while maintaining the shape and height of waveforms. Main constraint is the general polynomial fitting constraint; thus: $2M + 1 > N + 1$. Where M = impulse response half-length (window size) and N = polynomial order [6]. By appropriately choosing the values of M and N, the SGF was able to remove enough noise whilst maintaining the underlying pattern for each of the spectra measured. This approach allowed for accurate determination of the spacing between peaks.

The instability of the tunable laser causes the frequency sweeping to deviate from the intended range. This means that without calibration, the recorded spectrum may not accurately represent the true reflection characteristics of the device. This is why the Free Space Cavity (FSC) is needed. The FSC is mounted onto an optical table, which dampens out environmental vibrations which would cause changes in the free space length. Also, the FSC length is made long enough to make the Free Spectral Range (FSR) smaller and thus makes the frequency reference more precise. A free-space cavity is relatively simple to implement as it only requires two mirrors mounted to a table with an enclosure to block out ambient light and this is why FSC was used instead of fiber cavity. Also, the fiber cavity is more susceptible to temperature changes and it has a dispersion that has to be compensated. We know that, in the FSC, the spacing between the resonance frequencies (thus; the FSR) is 100 MHz. By using the known FSR of the FSC, we are able to effectively align the measured frequencies with the true frequencies, compensating for the nonidealities of the laser wavelength sweep. In order to align the measured frequencies with the true frequencies, we first have to identify the peaks in the FSC spectrum and readjust their positions so that the spacing between them will be uniform. The FSR of 100 MHz corresponds to ~800 fm in the wavelength domain at 1550 nm. The sweep width is obtained from the difference between maximum and minimum input wavelengths. Hence, number of peaks within the FSC spectrum is: sweep width/FSR in wavelength . During the wavelength sweep, a trigger signal from the laser was simultaneously recorded on the oscilloscope to indicate when the wavelength sweep of the laser started and ended. Therefore, the expected peak spacing within the FSC spectrum is: number of points within the sweep/number of peaks. Having calculated the expected peak spacing within the FSC, we used this value to check if the peaks we have identified in the FSC spectrum are the right peaks by taking the difference between the two. We expect the difference to be on the 0 line and Figure 2a shows this, where the peaks are correctly identified with only 3 outliers out of over 28,000 peaks. Figure 2b also shows the zoom-in plot of a portion of the first plot in Figure 2a, where the peaks have been identified correctly.

Having identified the peaks correctly, the algorithm for the frequency axis calibration is as follows:

1. Find the peaks in the FSC spectrum and their corresponding indices (index1)
2. Assuming first peak is start of the wavelength sweeping, then peak frequencies (F) are; $0\ to\ n * FSR$, in steps of FSR. Where n = number of identified peaks
3. Let indices of DUT spectrum (index2) = 1 to m, in steps of 1, m = length of DUT spectrum
4. Calibrated frequency axis = spline(index1, F, index2)

Where the spline function uses the third order (cubic) spline interpolation. Figure 3a shows the zoomed-in plot of the FSC spectrum before the frequency calibration, at different locations in the frequency axis. It clearly reveals the variation in peak spacing due to the instability in the tunable laser. Figure 3b also shows the zoomed-in plot of the FSC spectrum after the frequency calibration, at different locations in the frequency axis. It clearly shows no variation in peak spacing.

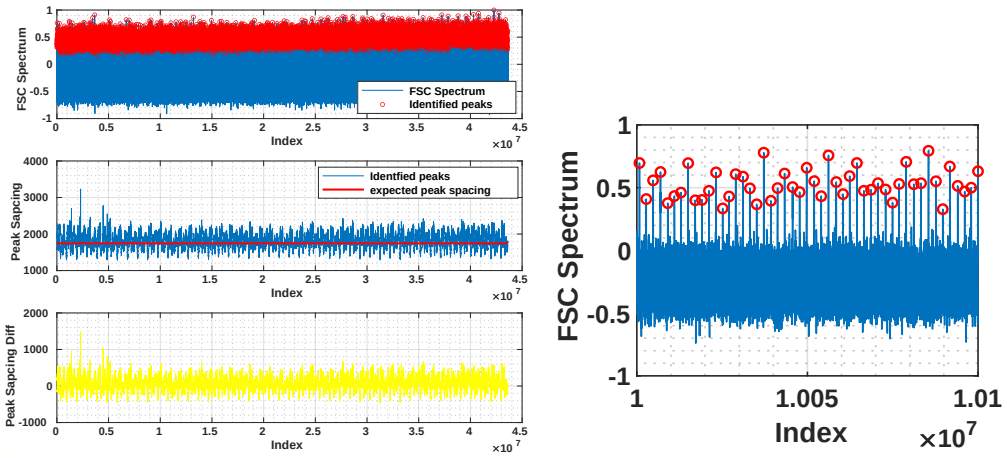

(**a**) (**b**)

Figure 2. (**a**) First plot at the top shows the FSC spectrum in blue and the identified peaks in red. Second plot in the middle shows the spacing between the peaks we identified in blue and the expected peak spacing in red. Last plot at the bottom shows the difference between the peak spacing we identified and the expected peak spacing, which is around the 0 value, suggesting that the peaks were correctly identified. (**b**) zoom-in on the first plot at the top in Figure 2a. It clearly shows the identified peaks.

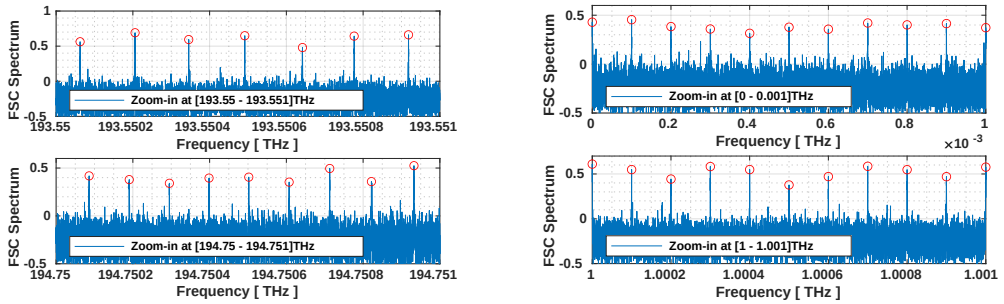

(**a**) (**b**)

Figure 3. (**a**) Zoomed-in plot of the FSC spectrum before the frequency calibration. It can be seen that the spacing between peaks in the portion of the plot at the top differs from the spacing between peaks in the portion of the plot at bottom. (**b**) Zoomed-in plot of the FSC spectrum after calibration, which reveals no variation in peak spacing.

Figure 4a shows a zoomed-in plot of the unfiltered spectrum from one of the DUT. Where it can be observed that, the rising and falling edges of the spectrum are relatively less noisy. It can also be observed that, while interference fringes are clearly measured, there is additional noise and zooming in reveals no periodicity except the one shown. Since there is no other periodicity, there are no reflections from other cavities, and the suspected noise is noise that comes from other sources, like from the detector. Figure 4b also shows a zoomed-in plot of the filtered DUT spectrum. We set a threshold to pass through the rising and falling edges of the spectrum. Using the points where the rising and falling edges intersect the threshold, we calculate the mid points between these two intersection points to get the frequency positions for the peaks. This approach was adopted because, even after filtering, there might be other residual features that hinder peak detection. By finding the spacing between the frequency positions of the peaks, the group delay can be calculated.

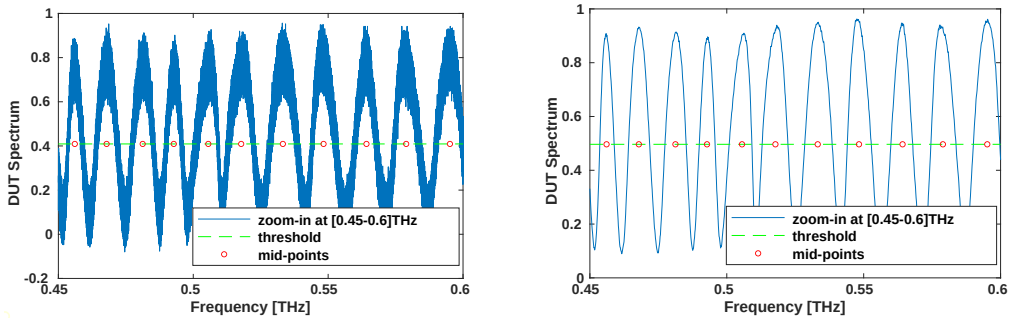

(**a**) (**b**)

Figure 4. (**a**) Zoomed-in plot of the unfiltered DUT spectrum, the threshold and the identified midpoints. (**b**) Zoomed-in plot of the filtered DUT spectrum, the threshold and the identified midpoints. It can be observed that peak spacing increases as frequency increases.

3. Results and Discussion

Based on the data measured, the above data analysis procedures have been used to calculate the group delay for the device. A total of 7 different measurements were taken using the experimental setup, by varying measurement parameters such as; input power, sample points, sweeping time, scanning speed, etc. One of the calculated group delay from the DUT is shown in Figure 5a, where for each parameters that were set, 9 different measurements were taken on the device and all 9 measurements plotted on the same graph. One of the parameter set to generate Figure 5a are; wavelength range = (1530–1550) nm, input power = −57 dBm, sample points = 50 MS, sweep time = 5 s, and scan speed = 11.1 nm/s. The group delay, as a function of frequency or wavelength is a linear function, with some additional oscillations. Again, the group delay ripple is usually observed experimentally [7,8], and in a particular case of chirped Bragg gratings, it is partly as a result of the perturbation induced in the effective index, which can be reduced by decreasing the corrugation width and also by careful apodization [9]. From the experimental data, the group delay was found to be noisy at low frequencies (which was as expected) and only the linear portion of the group delay was considered. This linear portion corresponds to the region where the DUT is intended to be used to provide linear dispersion within a photonic integrated circuit. Using the curve-fitting strategy, a linear fit was applied to the linear region of the group delay curve. The slope (which is the dispersion of the device) on the group delay curve for each of the 7 measurements was calculated. Figure 5b shows the plot of linear region of the group delay, where a linear fit was applied.

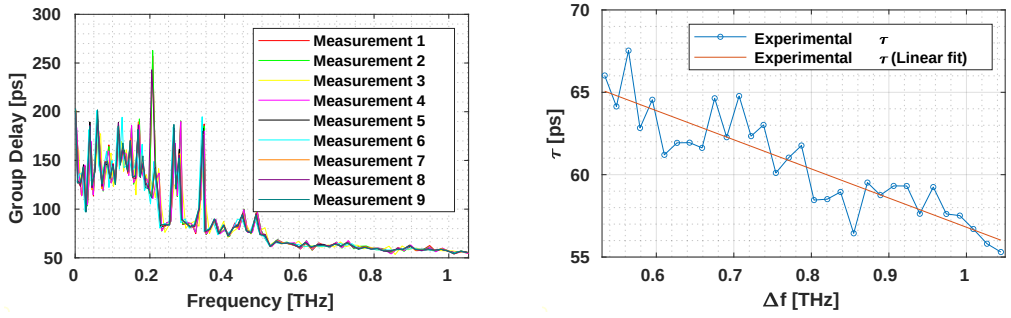

(**a**) (**b**)

Figure 5. (**a**) Calculated group delay for one of the DUT plotted on the frequency scale relative to the starting frequency. A total of 9 different measurements were taken on the same device and all 9 measurements plotted. (**b**) Linear curve fit at the linear region of Figure 5a.

Table 1 shows the experimentally measured dispersion for all 7 measurements that were taken. The DUT is a linearly chirped Bragg grating designed to generate a dispersion of $-45.9\ ps^2$. From the experimentally measured data, the dispersion of the device, fabricated on a silicon on insulator platform was found to be $-45.50 \pm 12\ ps^2$, which is in good agreement with the design dispersion value.

Table 1. Showing the experimentally measured dispersion for all 7 measurements that were taken.

Device Measurement	Dispersion [ps^2]
First Measurement	−59.45
Second Measurement	−41.15
Third Measurement	−35.14
Fourth Measurement	−35.49
Fifth Measurement	−40.95
Sixth Measurement	−65.79
Seventh Measurement	−40.53

4. Conclusions

Analyzing interferometric fringes from DUT light reflections offers a fast method for measuring the dispersion of integrated waveguide devices, which aligns well with design values. The consistency in the data analysis techniques have provided confidence in the validity of our measurements. In terms of how fast our method is, if we consider the programmable optical filter (used in [2]), an example is the waveshapers from Finisar. From the datasheet in [10], they have a settling time of 500 ms, (which means that each data point will take at least 500 ms to record) and the minimum step size is 8 pm. In the specific method that we are referring to, at least 4 filter shapes need to be applied. The wavelength range is 1530 nm–1550 nm = 20 nm. So total point is (20 nm/8 pm) $\times$ 4 and the total time is (20 nm/8 pm) $\times$ 4 $\times$ 0.5 s = 5000 s. Which is approximately 1 h 23 min. For our measurement technique, the sweeping time is 5 s, hence, our method is significantly faster than this established method. Also, for the established methods in [1,2], expensive devices such as VNAs and programmable optical filters are required whereas in our method, no such device is required. This approach of ours could serve as an alternative to established methods, which we will further verify in the future.

Author Contributions: Conceptualization; M.G. and P.D.G. Methodology; L.E.G. and I.Y. Software; I.Y. Validation; L.E.G. and P.D.G. Formal analysis; L.E.G. and I.Y. Investigation; P.D.G., L.E.G. and I.Y. Resources; M.G. Data curation; L.E.G. and I.Y. Writing—original draft preparation; I.Y. Writing—review and editing; L.E.G., P.D.G., M.G. and I.Y. Visualization; I.Y. Supervision; L.E.G., M.G., and P.D.G. All authors have read and agreed to the published version of the manuscript.

Funding: This research received no external funding.

Institutional Review Board Statement: Not applicable.

Informed Consent Statement: Not applicable.

Data Availability Statement: The data supporting the findings of this study are available from Technical University of Denmark. Data access may be granted upon reasonable request.

Conflicts of Interest: The authors declare no conflicts of interest.

Abbreviations

The following abbreviations are used in this manuscript:

DUT	Device Under Test
FSC	Free Space Cavity
FSR	Free Spectral Range
TL	Tunable Laser
PC	Polarization Controller
PD	Photo Detector
OSC	Oscilloscope
CIR	Circulator
PM	Power meter
SGF	Savitzky Golay Filter

References

1. Costa, B.; Mazzoni, D.; Puleo, M.; Vezzoni, E. Phase shift technique for the measurement of chromatic dispersion in optical fibers using LED's. *IEEE Trans. Microw. Theory Tech.* **1982**, *30*, 1497–1503. [CrossRef]
2. Bottrill, K.R.; Ettabib, M.A.; Demirtzioglou, I.; Marchetti, R.; Lacava, C.; Parmigiani, F.; Richardson, D.J.; Petropoulos, P. Spectral Difference Interferometry for the Characterization of Optical Media. *Laser Photonics Rev.* **2019**, *13*, 1900007. [CrossRef]
3. Cheung, C.S. An Investigation of Chirped Fibre Bragg Gratings Fabry-Pérot Interferometer for Sensing Applications. Ph.D. Thesis, Cranfield University, Bedford, UK, 2005.
4. Ready, J.F. *Industrial Applications of Lasers*; Elsevier: Amsterdam, The Netherlands, 1997.
5. Schwelb, O. Transmission, group delay, and dispersion in single-ring optical resonators and add/drop filters-a tutorial overview. *J. Light. Technol.* **2004**, *22*, 1380. [CrossRef]
6. Schafer, R.W. What is a savitzky-golay filter?[lecture notes]. *IEEE Signal Process. Mag.* **2011**, *28*, 111–117. [CrossRef]
7. Belai, O.V.; Podivilov, E.V.; Shapiro, D.A. Group delay in Bragg grating with linear chirp. *Opt. Commun.* **2006**, *266*, 512–520. [CrossRef]
8. Sumetsky, M.; Eggleton, B.J.; de Sterke, C.M. Theory of group delay ripple generated by chirped fiber gratings. *Opt. Express* **2002**, *10*, 332–340. [CrossRef] [PubMed]
9. Sun, Y.; Wang, D.; Deng, C.; Lu, M.; Huang, L.; Hu, G.; Yun, B.; Zhang, R.; Li, M.; Dong, J.; et al. Large group delay in silicon-on-insulator chirped spiral Bragg grating waveguide. *IEEE Photonics J.* **2021**, *13*, 1–5. [CrossRef]
10. Finisar. *WaveShaper 4000S Multiport Optical Processor*. Available online: https://www.xsoptix.com/data/finisar/ds_fnsr_instr_WaveShaper_4000S.pdf (accessed on 14 December 2024).